Contrast Source Inversion Regularized via Synthetic Experiments

Loreto Di Donato, Martina Bevacqua, Lorenzo Crocco *Senior Member, IEEE*,
and Tommaso Isernia, *Member, IEEE*

***Abstract*—The recombination of the scattering experiments results via suitable and simple preprocessing represents a novel and emerging paradigm for microwave imaging. As a matter of fact, the resulting synthetic experiments, if properly designed, can be used to enforce peculiar effects, which can be in turn exploited to tackle the inverse scattering problem more conveniently or reliably. In this paper, we present a first example of application of the synthetic experiments framework to the popular contrast source inversion method. In particular, relying on synthetic experiments capable to induce circularly symmetric contrast sources, we devise an original and effective regularized contrast source inversion scheme. In such a scheme, an additional penalty term is added to the usual cost functional, to account for the peculiar nature of the synthetic contrast sources. Results with simulated and experimental data are given to show the effectiveness of the proposed approach.**

***Index Terms*—Electromagnetic Inverse Scattering Problems, Synthetic Scattering Experiments, Linear Sampling Method, Microwave Imaging, Contrast Source Inversion.**

I. Introduction

INVERSE scattering problems are relevant to several applications of electromagnetic waves, which range from non destructive testing, to subsurface prospecting and biomedical imaging. However, to pursue the characterization of an unknown obstacle, a non-linear and ill-posed inverse problem has to be faced [1].

In this respect, a class of solution approaches that is broadly adopted is the one of modified gradient (MG) methods [2]–[6], in which the inverse problem is cast as the minimization of a cost function. Such a function depends on both the unknown contrast (that encodes the obstacle properties) and an auxiliary unknown, which can be the field in the imaging domain [2], [4] or the contrast source therein induced [3], [5], [6]. These methods do not require any approximation (but for the obvious discretization), nor an explicit solution of the forward problem at each step. Moreover, they allow to deal with a manageable degree of nonlinearity, thanks to the introduction of the auxiliary unknown.

However, similar to other non-linear inversion schemes, MG methods are based on local iterative optimization, so that they are prone to the occurrence of false solutions [4], [7]. As such, ongoing efforts have been and are still devoted to devise regularization strategies [8] to defeat such a problem. For instance, widely adopted and effective schemes are the Tikhonov regularization [8], the multiplicative regularization [9], the total variation [10] and regularization by projection methods, in which the unknowns are represented by the coefficients of a suitable projection basis [11]–[13].

The above mentioned schemes enforce the regularization by imposing constraints on the contrast function. This implies that the choice of the most suitable scheme in some sense depends on the expected contrast properties (for instance, smoothness, piece-wise behavior and so on). In this paper, we explore a novel and different strategy, in which the problem is regularized by acting on the auxiliary unknown.

Such an alternative strategy is suggested by an emerging paradigm for inverse scattering, which consists in taking advantage of experiments that are designed in such a way to enforce some specific property of the field or the contrast source [14]–[17]. Notably, these experiments are implemented in a synthetic way, that is without performing additional or particular measurements, but processing the available ones. Accordingly, the approach does not rely on the availability of a priori information.

In particular, with respect to the canonical 2D scalar inverse scattering problem, we exploit this new concept in the framework of the popular contrast source inversion (CSI) scheme, by considering virtual experiments designed in such a way that the induced contrast sources exhibit circular symmetry properties and enforcing this property in the minimization process, through a suitably defined penalty term. As shown in the following, this leads to a new and effective regularized CSI strategy, which does not require a priori information and can successfully tackle different kind of targets.

The paper is organized as follows. In Section II, the inverse scattering problem is formulated, the CSI is recalled. In Section III, the concept of synthetic experiments introduced. In Section IV, we give criteria and tools to design the required synthetic experiments. In Section V, we introduce the new regularized CSI approach, whose performance are assessed with reference to both simulated and experimental data in Section VI. Conclusions follows. Throughout the paper, the time harmonic factor $exp(j\omega t)$ is omitted.

*This is the post-print version of the following article: L. Di Donato, M. T. Bevacqua, L. Crocco and T. Isernia, "Inverse Scattering Via Virtual Experiments and Contrast Source Regularization," in IEEE Transactions on Antennas and Propagation, vol. 63, no. 4, pp. 1669-1677, April 2015.
doi: 10.1109/TAP.2015.2392124. Article has been published in final form at: https://ieeexplore.ieee.org/document/7010008.*

II. Statement of the problem and CSI inversion scheme

Let $D \subseteq \Re^2$ denote the investigation domain that contains the cross-section Σ of one or more dielectric non-magnetic scatterers, whose properties are related to those of the homogeneous host medium through the contrast function:

$$\chi(\underline{r}) = \epsilon_s(\underline{r})/\epsilon_b - 1,$$

wherein $\underline{r} = (x, y)$, and ϵ_s and ϵ_b are the relative (possibly complex) permittivity of the scatterer and the background medium, respectively.

By assuming the TM polarization for the electric field, the equations governing the scattering phenomenon for the geometry at hand can be expressed in an integral form by means of the contrast source formulation as follows:

$$\begin{aligned} E_s(\underline{R}_m, \underline{R}_t) &= \int_D G(\underline{R}_m, \underline{r}')J(\underline{r}', \underline{R}_t)d\underline{r}' \\ &= \mathcal{A}_{\mathcal{R}}[J], \quad \underline{R}_m \in \Gamma_R, \end{aligned} \tag{1}$$

$$\begin{aligned} J(\underline{r}, \underline{R}_t) - \chi(\underline{r})E_i(\underline{r}, \underline{R}_t) &= \chi(\underline{r}) \int_D G(\underline{r}, \underline{r}')J(\underline{r}', \underline{R}_t)d\underline{r}' \\ &= \chi(\underline{r})\mathcal{A}_{\mathcal{D}}[J], \quad \underline{r} \in D, \end{aligned} \tag{2}$$

wherein E_i is the incident field radiated by a source positioned in $\underline{R}_t = (R, \theta) \in \Gamma_T$, with Γ_T being a curve external to D, E_s is the corresponding scattered field as measured at $\underline{R}_m = (R, \phi) \in \Gamma_R$, with Γ_R being a curve external to D, J is the current induced in D by E_i (i.e., the contrast source) and G is the Green's function, which, for the 2D case at hand, reads $G(\underline{r}, \underline{r}') = \frac{-j}{4}k_b^2 H_0^{(2)}(k_b|\underline{r} - \underline{r}'|)$, k_b being the wave-number in the host medium and $H_0^{(2)}$ being the zero order second kind Hankel function. The Green's function is the kernel of the radiation operators $\mathcal{A}_{\mathcal{R}}[\cdot] : L^2(D) \rightarrow L^2(\Gamma_R)$ and $\mathcal{A}_{\mathcal{D}}[\cdot] : L^2(D) \rightarrow L^2(D)$ that relate the contrast sources in D to the field they radiate on Γ_R and in D, respectively.

The inverse scattering problem aims at retrieving the unknown contrast χ for $\underline{r} \in D$ from the scattered fields E_s measured for several receiving positions $\underline{R}_m$ induced by the set of known incident fields E_i radiated by several source positions $\underline{R}_t \in \Gamma$. As well known, such a problem is non-linear and ill-posed. The former property descends from the dependance of the contrast source J on the unknown contrast function χ, while the latter on the compactness of the radiation operator $\mathcal{A}_{\mathcal{R}}$.

In particular, due to ill-posedness, only a finite number of independent experiments (and measurements) is available and only a limited number of independent parameters can be recovered from scattered field data [18]–[20]. Accordingly, we will consider from now on a finite number, say N, of scattering experiments. In so doing, care has to be taken in choosing the probes' positions $R_t^1, ...R_t^N$ and $R_m^1, ...R_m^N$, in such a way to collect in a non redundant fashion all the available information. This can be efficiently done by adopting the measurement strategies proposed in [18], wherein a Nyquist criterion is essentially suggested.

The CSI scheme tackles the problem looking for both the unknown contrast χ and the auxiliary unknown J. In particular, the problem's solution is defined as the global minimum of the cost functional:

$$\begin{aligned} \Phi_{CS}(\chi, J^{(1)}, ..., J^{(N)}) = &\sum_{v=1}^{N} \frac{\|E_s^{(v)} - \mathcal{A}_{\mathcal{R}}[J^{(v)}]\|^2}{\|E_s^{(v)}\|^2} \\ &+ \sum_{v=1}^{N} \frac{\|J^{(v)} - \chi E_i^{(v)} - \chi\mathcal{A}_{\mathcal{D}}[J^{(v)}]\|^2}{\|E_i^{(v)}\|^2}. \end{aligned} \tag{3}$$

III. Synthetic experiments as a way to re-weight the measured information

Although the formulation given in the previous Section is the typical and mostly used one, an interesting circumstance descends from the inherent linearity of the scattering phenomenon for a fixed contrast function. According to this property, a superposition of the incident fields gives rise to a scattered field which is nothing but the same superposition of the corresponding scattered fields. In fact, if we consider a superposition of incident fields given by:

$$E_i^{(s)}(\underline{r}) = \sum_{n=1}^{N} \alpha_n E_i(\underline{r}, \underline{R}_t), \tag{4}$$

where $E_i(\underline{r}, \theta_n)$ are the original incident fields coming from the N different directions θ_n, the incident field (4) will give rise to the contrast source:

$$J^{(s)}(\underline{r}) = \sum_{n=1}^{N} \alpha_n J(\underline{r}, \underline{R}_t), \tag{5}$$

and, finally, this latter will produce the scattered field

$$E_s^{(s)}(\underline{R}_m) = \sum_{n=1}^{N} \alpha_n E_s(\underline{R}_m, \underline{R}_t). \tag{6}$$

Accordingly, performing several re-arrangements of the original experiments, it is possible to build a set of new experiments. We will refer to these new experiments as "synthetic" or "virtual" experiments, to remark that they do not require further experimental measurements, but can be generated through software processing.

Obviously, synthetic experiments are just a different way to consider, or saying it better, to "re-weight" the originally collected information, so that the above mentioned issues on the finite amount of independent information available to solve the inverse problem still hold true[1].

Nevertheless, as long as they are properly designed, one can tackle the original problem in terms of synthetic experiments rather than reasoning in terms of original ones. For instance in [14] and [17], this concept has been used to devise new approximeted inversion methods that can allow an effective solution of the problem. In the following, we apply this concept to the CSI framework, by considering virtual experiments capable to enforce contrast sources having an a priori given structure, designed according to the criterion discussed in the next Section.

[1] Actually, care has to be taken in generating synthetic experiments in order to avoid loss of significant information.

IV. Synthesizing circularly symmetric contrast sources

The aim of this Section is to devise a strategy to design a set of synthetic experiments, which does not rely on a priori information. To this end, the scattered fields collected in the original experiments are the only degree of freedom and have to be somehow processed to achieve the desired result.

As a possible choice, we aim to enforce a circular symmetry of the scattering phenomenon around given points. That is, we pursue the design of virtual experiments such that each one of the resulting scattered fields exhibits (within some required accuracy) a circular symmetry around some "pivot" point, say $\underline{r}_p$.

Such a goal can be accomplished by requiring that the original scattered fields should fulfill the following equation:

$$\sum_{n=1}^{N} \alpha_n^p E_s(\underline{R}_m, \underline{R}_t) = \sqrt{\frac{2}{\pi k_b |\underline{R}_m - \underline{r}_p|}} e^{-\jmath k_b |\underline{R}_m - \underline{r}_p|}, \quad (7)$$

where $A_p = \{\alpha_1^p, ..., \alpha_N^p\}$ identify the combination coefficients required to implement the synthetic scattering experiments that give raise to the sought circular symmetry around the considered pivot point $\underline{r}_p$. In fact, assuming that one is able to determine these coefficients, by virtue of eqs. (4)-(6), they also define the incident field that gives rise to the contrast source radiating such a scattered field.

Interestingly, eq. (7) is nothing but the discretized version of the well-known "far field" equation, i.e., the basic (linear) equation underlying the linear sampling method (LSM) [21], with $\underline{r}_p$ playing the role of the *sampling* point. Accordingly, the problem cast in (7) is ill-conditioned and has to be solved through some regularization strategy.

Here, we adopt the Tikhonov regularization, which has also an effect on the synthesized contrast source. In fact, the minimum energy requirement (on the primary sources) enforced by the Tikhonov regularization corresponds to minimize the non radiating component of the contrast sources [22]. As a consequence, as long as eq. (7) is fulfilled (in a regularized sense), the resulting synthetic contrast source will exhibit an essentially circularly symmetric structure with respect to the pivot point at hand.

Taking the above circumstance into account, in the following we present a new regularization scheme for CSI, in which the scattering problem is recast into a set of synthetic experiments (rather than the original multi-view multi-static ones) and circularly symmetric contrast sources are looked for. Notably, such an assumption entails that circularly symmetric non radiating sources are also taken into account in the model, while angularly varying (radiating and non radiating) contrast sources are instead neglected, being they expected to be small.

V. A New Regularized Contrast Source Inversion Strategy

Let us assume that eq. (7) has been applied to the whole imaging domain D. Then, let $r_p^1, ..., r_p^P$ be a set of P pivot points for which the equation has been solved (in a regularized sense) and denote with $A_1, ..., A_P$ the sets of corresponding coefficients.

Now, it is possible to recast the original problem given in eqs. (2) and (1), in terms of the obtained synthetic scattering experiments, in which a circular symmetry of the contrast sources around the selected pivot points is expected.

To this end, we define the set of synthetic incident fields:

$$\Psi_i^{(p)}(\underline{r}) = \sum_{n=1}^{N} \alpha_n^p E_i(\underline{r}, \underline{R}_t), p = 1, ..., P, \quad (8)$$

which, by construction, give raise to scattered fields that approximate cylindrical waves emanating from the generic r_p, i.e.,

$$\Psi_s^{(p)}(\underline{R}_m) = \sum_{n=1}^{N} \alpha_n^p E_s(\underline{R}_m, \underline{R}_t), p = 1, ..., P. \quad (9)$$

With respect to the synthetic experiments devised above, we can cast the CSI scheme as the minimization of the cost function:

$$\begin{aligned} \Phi_0(\chi, J^{(1)}, ..., J^{(P)}) &= \Phi_{CS}(\chi, J^{(1)}, ..., J^{(P)}) \\ &+ \Phi_1(J^{(1)}, ..., J^{(P)}), \end{aligned} \quad (10)$$

wherein the first term is the CSI functional (3) as cast for the synthetic fields in (8) and (9), while the third term acts as a regularizing constraint, meant to enforce the expected contrast sources properties by minimizing the angular variation of each $J^{(p)}$ around the pertaining pivot point $\underline{r}_p$:

$$\Phi_1 = \sum_{p=1}^{P} \tau_p \Pi_p \left\| \frac{\partial J^{(p)}}{\partial \phi_p} \right\|^2. \quad (11)$$

In (11), $\{\tau_p\}_1^N$ are non negative parameters controlling the relative weight of such a regularization term and ϕ_p is the angular coordinate of the local reference system centered on the pivot points. Finally, Π_p is a circular support mask function that forces the penalty term to act only in a neighborhood of the pivot point.

The minimization of the cost function is carried by simultaneously updating both the contrast and the contrast source, using the same scheme as in [4]. Details about implementation of such a regularization term in the framework of a gradient-projection optimization are reported in the Appendix, while criteria for the choice of the pivot points $\underline{r}_p$, the parameters τ_p and mask functions Π_p are discussed below.

A. On the choice of $\underline{r}_p$, Π_p and τ_p

The choice of the parameters takes advantage of the capability of LSM to estimate the support of the scatterers, by simply plotting the "indicator" function $||A_p||$ for all the points in which (7) has been solved.

From this circumstance, it follows that the condition to choose the pivot points $\underline{r}_p$ is that they belong to such an estimated support. In particular pivot points evenly spaced over this region can be conveniently chosen to ensure probing diversity, while avoiding any significant loss of information [14].

To select the suitable radius of Π_p, we recall that the contrast source must have the same support Σ as the scatterer [23], [24]. Hence, the maximum allowed value for the radius of Π_p will be ruled by the distance between $\underline{r}_p$ and the estimated boundary of the scatterer. Note this means that mask functions of different radius (and extent) will be adopted for the different pivot points, depending on the distance from the boundary. In particular, the closer the pivot point to the (estimated) borders of the scatter, the smaller the radius of the corresponding mask function Π_p.

Similar arguments can be exploited for the choice of τ_p. In particular, since the contrast source's support is constrained onto Σ, we expect that the induced current for $\underline{r}_p$ close to the estimated boundary does not show an exact circular symmetry (with respect to $\underline{r}_p$) [23], [24]. This physical observation corresponds to what is foreseen by LSM theory, according to which the energy of the solution $||A_p||$ blows up when $\underline{r}_p$ approaches the boundary of the scatterer [25]. Accordingly, we can devise an automatic way to select τ_p by relying on the value of $||A_p||$ in $\underline{r}_p$. In particular, we compute the logarithmic value[2] of $||A_p||$ as normalized over the whole imaged domain, and set τ_p equal to the value obtained in the relevant $\underline{r}_p$. Note, this allows to set values of τ_p in the range $]0, 1]$.

VI. Inversion results

A. Simulated data

This section reports some examples with synthetic data to assess the performance of the proposed inversion strategy. For all the examples, the scattered field data are collected under a multiview-multistatic configuration, wherein the probed area is a square region of side L_D embedded in homogeneous background. In order to properly sample the scattered field, we consider a number of measurements points equal to the minimum non redundant number of independent scattering experiments, which is given by $M_D = 2Re[k_b]a_D + 1$, a_D being the radius of the minimum circle enclosing the investigated scenario [18] and k_b the wave number in the host medium. Without loss of generality the background medium is the vacuum for all the examples and the primary sources are filamentary currents. Accordingly, the number of receivers and transmitters, angularly evenly spaced on a circumference of radius R, is set equal to M_D [18].

The scattered field data have been simulated by means of a full-wave forward solver based on the MoM and corrupted with a random gaussian noise with prescribed SNR level. The reconstruction's accuracy is appraised in terms of the mean square error (MSE):

$$MSE = \frac{\sum_{k=1}^{N_c} |\chi_k - \widetilde{\chi}_k|^2}{\sum_{k=1}^{N_c} |\chi_k|^2} \qquad (12)$$

where N_c is the number of cells of the domain under investigation, χ is the actual contrast profile and $\widetilde{\chi}$ is the reconstructed one.

For the sake of comparison, we also performed the inversion using two alternative strategies, in which the regularization of the CSI functional (3) is enforced by projecting the unknown contrast profile onto the spatial Fourier harmonics basis [4], [26]. In particular, we apply this regularization to both the CSI scheme cast in terms of the original experiments and in terms of the synthetic ones. In both cases, the number of sought unknown Fourier coefficients is set equal to the degrees of freedom [18] corresponding to the estimated scatterer support. In all cases, the back-propagation solution has been used as starting guess of the iterative minimization.

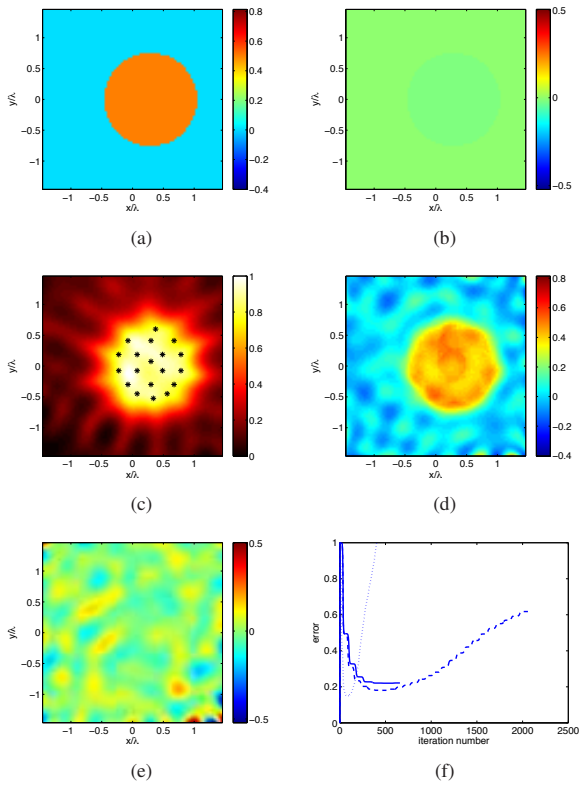

Fig. 1. Imaging results for the example 1. (a) Real and (b) imaginary parts of the actual contrast profile; (c) Shape estimate by means of the normalized logarithmic LSM indicator: the pivot points chosen for quantitative inversion are marked with a star. (d) Real and (e) imaginary part retrieved with the proposed regularization strategy, (f) MSE at each iteration for the proposed strategy (continuous line), for CSI inversion of the original experiments regularized with projection onto Fourier harmonics (dotted line), and for the CSI functional cast for the synthetic experiments regularized by projections (dash-dotted line).

In order to build the synthetic scattering experiments and cast the corresponding scattering equations, the scattered field data are first processed by solving the far field equation (7) onto an arbitrary grid of points that samples the imaging domain D. In so doing, the same Tikhonov parameter is taken for all points and fixed following the guidelines in [27]. Then, the pivot points' locations are chosen from the estimated support, given by normalized logarithmic plot of $||A_p||$ over D.

In the first example we have considered a large circular scatterer with diameter of 1.5λ, Fig.1. The dielectric permittivity is $\epsilon_s = 1.5$ while $\sigma = 0.02\ S/m$. Furthermore,

[2]The logarithm allows to emphasize the energy variation amongst the different pivot points.

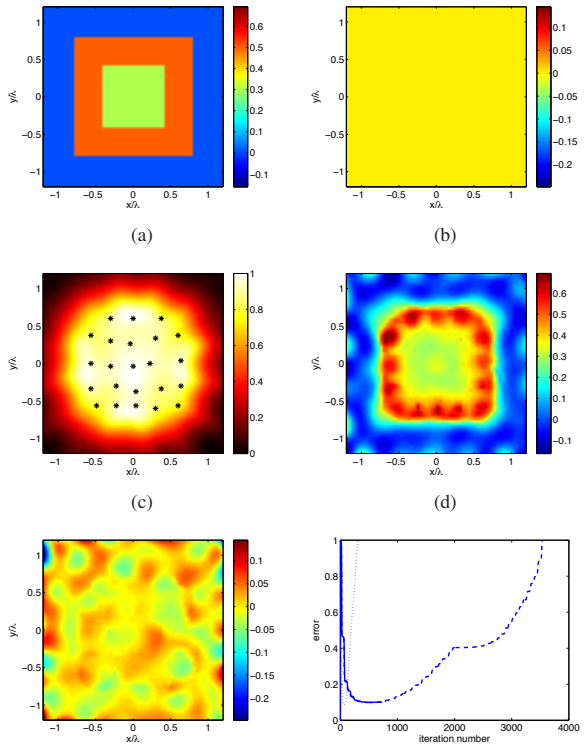

Fig. 2. Imaging results for the example 2. (a) Real and (b) imaginary parts of the actual contrast profile; (c) Shape estimate by means of the normalized logarithmic LSM indicator: the pivot points chosen for quantitative inversion are marked with a star. (d) Real and (e) imaginary part retrieved with the proposed regularization strategy, (f) MSE at each iteration for the proposed strategy (continuous line), for CSI inversion of the original experiments regularized with projection onto Fourier harmonics (dotted line), and for the CSI functional cast for the synthetic experiments regularized by projections (dash-dotted line).

$N_c = 78 \times 78$, $M = N = 31$, $R = 8\lambda_b$, $L_D = 3\lambda_b$, where λ_b is the wavelength in the host medium at 5GHz. Finally, the simulated data have been corrupted by a simulated error ($SNR = 10dB$). The LSM indicator is shown in Fig. 1(c), wherein the selected pivot points are also marked. According to the guidelines given in the previous Section, the radius of the mask function Π_p is set to $0.3\lambda_b$ for the 12 pivot points closer to the boundary, $0.5\lambda_b$ for the inner pivot points and $0.65\lambda_b$ for the central one. The corresponding reconstruction is shown in Figs. 1(d)-(e). Notably, while the MSE using the proposed approach is as low as $err = 22\%$ (after 658 iterations), the iterative procedure (looking for 12×12 Fourier harmonics) diverges after a few iterations for the original scattering experiments' data and reaches an error of about 60% for the pre-processed synthetic ones, Fig.1(f).

In the second example, a large square scatterer has been considered, see Fig. 2. The inner square has $\epsilon = 1.3$ and the outer square has $\epsilon = 1.5$, while $N_c = 64 \times 64$, $M = N = 25$, $R = 5.35\lambda_b$, $L_D = 2.4\lambda_b$, $SNR = 20dB$ at 800MHz. Following the same steps as above, the results summarized in Fig. 2 are achieved. In this case, the values of the radius for Π_p have been set to $\lambda_b/4$ (14 pivot points), $\lambda_b/3$ (9 p.p.), $\lambda_b/2$ (1 p.p.) for the pivot points from the borders to the center of the retrieved scatterer support. Also in this case, see Figs. 2(f), the proposed approach converges to a low MSE (err=10%) while the two other methods diverge (looking for 16×16 harmonic coefficients).

As a last example, we have considered the dielectric lossy ring shown in Fig.3(a)-(b). As well known, such a kind of target represents a very unfavorable case for the LSM [**?**], [21]. As a matter of fact, due to multiple connection of the support and the circular symmetry of the contrast profile, the LSM fails in retrieving the actual support [?], but can only provide an image of the convex hull, as indeed shown in Fig.3(c). Nevertheless, the proposed strategy is still successful, even if this example clearly represents a critical situation. In particular, by relying on the (inaccurately) estimated support, we have selected the pivot points shown in Fig.3(c), that are indeed not all located within Σ. Then, following the guidelines given in Sec. V-A, we have set the mask functions Π_p shown in Fig.3(d)-(f), having radius $\lambda_b/2$, $\lambda_b/3$, and $\lambda_b/6$, respectively and performed the regularized CSI inversion. The final achieved result is shown in Figs. 3(g)-(h), that correspond to an MSE of 21%. The parameters for this example are $\epsilon = 1.5$, $N_c = 64 \times 64$, $M = N = 25$, $R = 5.33\lambda_b$, $L_D = 2.4\lambda_b$, $SNR = 20dB$ at 800MHz.

B. Experimental data

To assess the proposed approach against experimental data, we have considered the $TwinDielTM$ of the 2001 Fresnel data-set [28]. The test bed is made of two identical cylinders having radius 1.5cm and relative permittivity 3 ± 0.3. The data have been measured under a partially aspect limited configuration, in which the illuminations completely surround the targets, but, for each illumination, the measurements are taken only on an angular sector of 240 degrees. In particular, the original collected data consists of 36 illumination directions and 49 measurements for each view. The complete description of the targets and the measurement set-up can be found in [28].

We have processed single frequency data at 5GHz. The LSM image for the two dielectric cylinders is shown in Fig.4. Such a result has been achieved by adopting a 36×36 multiview-multistatic data matrix in which the data entries not available have been replaced with zeros. As can be seen, the targets' s shape is properly estimated so that the pivot points can be properly chosen, see Fig. 4(a). In particular, 18 pivot points are set to rearrange the scattered fields and the primary fields, the latter being expressed trough a multipole expansion according to the procedure suggested in [29]. As can be noticed, even if no a priori information on the target's nature have been enforced, the dielectric permittivity value is accurately (i.e quantitatively) retrieved, see Figs. 4(b). It is worth to underline that also in this case the projection regularized CSI schemes diverge.

VII. Conclusions

In this paper, we have presented a CSI scheme in which the regularization is enforced on contrast sources induced by

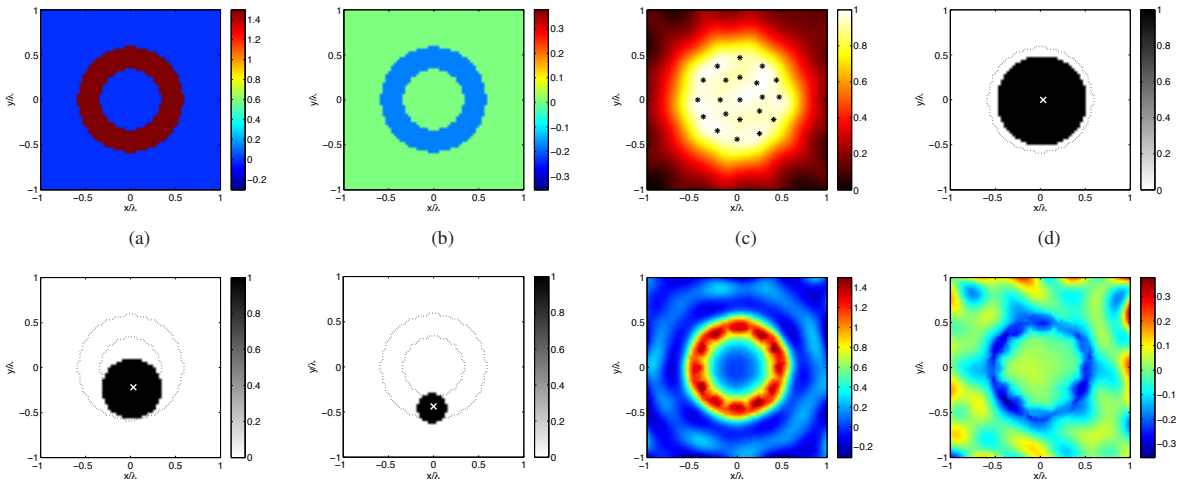

Fig. 3. Imaging results for the example 3. (a) real part and (b) imaginary part of the contrast profile; (c) LSM image, wuth the selected pivot points superimposed on it; (d) mask functions Π_p for the central pivot point, (e) Π_p for the inner ring of pivot points, (f) Π_p for the outer ring of pivot points, a contour plot of the actual scatterer support is also depicted. Reconstruction results with the proposed inversion strategy, (g) real part of the retrieved contrast, (h) imaginary part of the retrieved contrast.

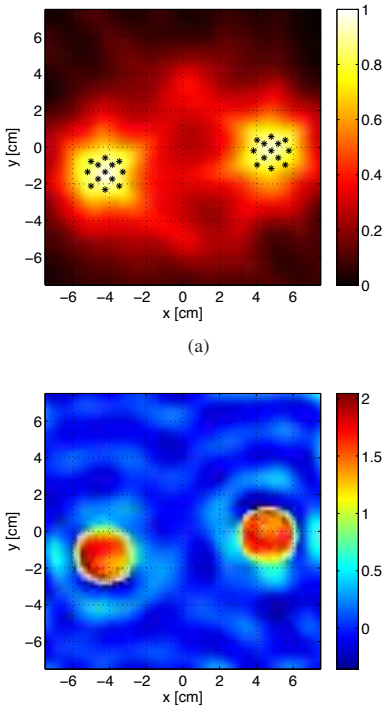

Fig. 4. Imaging results for the $TwinDielTM$ data-set: (a) the LSM indicator and the selected pivot points; (b) real part of the retrieved contrast profile.

means of suitably designed synthetic experiments. Besides offering a different, possibly complementary, point of view to regularize the inversion, as compared to usual methods that act on the contrast function, the paradigm underlying this contribution opens the way to new ways to tackle the inverse scattering problem. For instance, such a strategy has been indeed exploited in [14] and [17] , where new and effective approximated inversion methods have been proposed. In this respect, an interesting extension of the present work is the application of this regularization framework to the contrast source extended Born model [5], an alternative source type model that is in some sense complementary to CSI [30]. Also, the exploitation of different kind of field symmetries, enforced by means of the generalized LSM formulation [24] are worth to be pursued, together with the extension of the concept to the $3D$ vectorial case.

APPENDIX

We analytically derive the expression for the gradient and the line search parameter related to the term (11) in a conjugate gradient scheme following the approach in [4].

First, let us observe that the third part of the functional to be minimized depends only on the auxiliary unknown $J^{(p)}$. Defining the functional to be minimized as $\mathcal{F}[x^{(1)},...,x^{(P)}]$ and $\triangle J^{(p)}$ the variation due to an increment of $\triangle x^{(p)}$, the corresponding variation of the functional is given by:

$$\triangle \mathcal{F}_{x^{(p)}} = \left\{ \langle \frac{\partial J^{(p)}}{\partial \phi_p}, \frac{\partial \triangle J^{(p)}}{\partial \phi_p} \rangle \right\} + c.c. \qquad (A.1)$$

where $\langle \cdot, \cdot \rangle$ denotes usual scalar product, and c.c. stands for conjugate of the first addendum. Taking into account the the properties of the involved differential operator [31], (A.1) can be rewritten as

$$\triangle \mathcal{F}_{x^{(p)}} = \left\{ \langle -\frac{\partial^2 J^{(p)}}{\partial \phi_p^2}, \triangle J^{(p)} \rangle \right\} + c.c. \qquad (A.2)$$

and therefore, $\nabla\mathcal{F}_{x^{(p)}}$ being such that $\triangle\mathcal{F}_{x^{(p)}} = \langle\nabla\mathcal{F}_{x^{(p)}}, \triangle x^{(p)}\rangle$:

$$\nabla\mathcal{F}_{x^{(p)}} = 2\left(-\frac{\partial^2 J^{(p)}}{\partial\phi_p^2}\right) \tag{A.3}$$

Let us consider the behavior of functional (11) along an arbitrary line whose direction is given by $J^{(p)} + \lambda\nabla J^{(p)}$ so that

$$\nabla\mathcal{F}[x^{(p)} + \lambda\nabla x^{(p)}] = \\ = \sum_{p=1}^{P}\left\{\langle\frac{\partial J^{(p)}}{\partial\phi_p} + \lambda\frac{\partial\triangle J^{(p)}}{\partial\phi_p}, \frac{\partial J^{(p)}}{\partial\phi_p} + \lambda\frac{\partial\triangle J^{(p)}}{\partial\phi_p}\rangle\right\} \tag{A.4}$$

Due to the nature of the involved operator, (A.4) can be rewritten as a second degree algebraic polynomial, i.e.

$$f(\lambda) = c_2\lambda^2 + c_1\lambda + c_0 \tag{A.5}$$

where

$$c_2 = \sum_{p=1}^{P}\left\|\frac{\partial\triangle J^{(p)}}{\partial\phi_p}\right\|^2 \tag{A.6}$$

$$c_1 = 2Re\sum_{p=1}^{P}\left\{\langle\frac{\partial J^{(p)}}{\partial\phi_p}, \frac{\partial\triangle J^{(p)}}{\partial\phi_p}\rangle\right\} \tag{A.7}$$

$$c_0 = \sum_{p=1}^{P}\left\|\frac{\partial J^{(p)}}{\partial\phi_p}\right\|^2 \tag{A.8}$$

REFERENCES

[1] D. Colton and R. Kress. *Inverse Acoustic and Electromagnetic Scattering Theory*. Springer-Verlag, Berlin, Germany, 1992.

[2] R. E. Kleinman and P. M. van den Berg. An extended modified gradient technique for profile inversion. *J. Geophys. Res.*, 28(2):877–884, 1993.

[3] P. M. van den Berg and R. E. Kleinman. A contrast source inversion method. *Inv. Probl.*, 13(6):1607–1620, 1997.

[4] T. Isernia, V. Pascazio, and R. Pierri. A nonlinear estimation method in tomographic imaging. *IEEE Trans. Geosci. Remote Sens.*, 35:910–923, 1997.

[5] T. Isernia, L. Crocco, and M. D' Urso. New tools and series for forward and inverse scattering problems in lossy media. *IEEE Trans. Geosci. Remote Sens. Lett.*, 1(4):327–331, 2004.

[6] X. Chen. Subspace-based optimization method for solving inverse-scattering problems. *IEEE Transactions on Geoscience and Remote Sensing*, 48(1):42–49, Jan 2010.

[7] T. Isernia, V. Pascazio, and R. Pierri. On the local minima in a tomographic imaging technique. *IEEE Trans. Geosci. Remote Sens.*, 39:1596–1607, 2001.

[8] M. Bertero. Linear inverse and ill-posed problems. *Adv. Electron. Phys.*, 75:1–120, 1989.

[9] Peter M. van den Berg, Aria Abubakar, and Jacob T. Fokkema. Multiplicative regularization for contrast profile inversion. *Radio Science*, 38(2):n/a–n/a, 2003.

[10] P M van den Berg and R E Kleinman. A total variation enhanced modified gradient algorithm for profile reconstruction. *Inverse Problems*, 11(3):L5, 1995.

[11] I. Catapano, L. Di Donato, L. Crocco, O. M. Bucci, A. F. Morabito, T. Isernia, and R. Massa. On quantitative microwave tomography of female breast. *Prog. Electromagn. Res.*, 97:75–93, 2009.

[12] R. Scapaticci, I. Catapano, and L. Crocco. Wavelet-based adaptive multiresolution inversion for quantitative microwave imaging of breast tissues. *Antennas and Propagation, IEEE Transactions on*, 60(8):3717–3726, Aug 2012.

[13] A. Abubakar M. Li, O. Semerci. A contrast source inversion in the wavelet domain. *Inverse Problems*, 29(2):025015 (19pp), 2013.

[14] L. Crocco, I. Catapano, L. Di Donato, and T. Isernia. The linear sampling method as a way for quantitative inverse scattering. *IEEE Trans. Antennas Propag.*, 4(60):1844–1853, 2012.

[15] Di Donato L., Bevaqua M., Isernia T., Catapano I., and Crocco L. Improved quantitative microwave tomography by exploiting the physical meaning of the linear sampling method. In *Proc. of the Antennas and Propagation (EuCAP), 2012 5-th European conference on*, pages 3828–3831, 11-15 Apr., 2012. IEEE.

[16] Crocco L., Catapano I., Di Donato L., and Isernia T. Enhancing the factorization method relying on its physical meaning. In *Proc. of the Antennas and Propagation (EuCAP), 7-th European conference on*, 8-12 Apr. 2013.

[17] M. Bevacqua, L. Crocco, L. Di Donato, and T. Isernia. An algebraic inversion method for non-linear inverse scattering. *IEEE Trans. Antennas Propag.*, Submitted.

[18] O. M. Bucci and T. Isernia. Electromagnetic inverse scattering: retrievable information and measurement strategies. *Radio Sci.*, 32:2123–2138, 1997.

[19] O. M. Bucci and G. Franceschetti. On the spatial bandwidth of the scattered fields. *IEEE Trans. Antennas Propag.*, 35(12):1445–1455, 1987.

[20] O. M. Bucci and G. Franceschetti. On the degrees of freedom of scattered fields. *IEEE Trans. Antennas Propag.*, 37(7):918–926, 1989.

[21] F. Cakoni and D. Colton. *Qualitative methods in inverse scattering theory*. Springer-Verlag, Berlin, Germany, 2006.

[22] Crocco L., Di Donato L., Iero D. A. M., and Isernia T. An adaptive method to focusing in unknown scenario. *Progress in Electromagnetic Research*, 130:563–579, 2012.

[23] I. Catapano, L. Crocco, and T. Isernia. On simple methods for shape reconstruction of unknown scatterers. *IEEE Trans. Antennas Propag.*, 55:1431–1436, 2007.

[24] L. Crocco, L. Di Donato, I. Catapano, and T. Isernia. An improved simple method for imaging the shape of complex targets. *IEEE Trans. Antennas Propag.*, 2:843–851, 2013.

[25] D. Colton, H. Haddar, and M. Piana. The linear sampling method in inverse electromagnetic scattering theory. *Inverse Probl.*, 19:105–137, 2003.

[26] L. Crocco O. M. Bucci A. F. Morabito T. Isernia R. Massa I. Catapano, L. Di Donato. On quantitative microwave tomography of female breast. *Progress In Electromagnetics Research - PIER*, 97:75–93, 2009.

[27] I. Catapano and L. Crocco. An imaging method for concealed targets. *IEEE Trans. Geosci. Remote Sens.*, 47(5):1301–1309, 2009.

[28] K. Belkebir and M. Saillard. Guest editors' introduction. *Inverse Probl.*, 17:1565.

[29] L. Crocco and T. Isernia. Inverse scattering with real data: detecting and imaging homogeneous dielectric objects. *Inverse Probl.*, 17(6):1573, 2001.

[30] M. D' Urso, T. Isernia, and A. F. Morabito. On the solution of 2D inverse scattering problems via source-type integral equations. *IEEE Trans. Geosci. Remote Sens.*, 13(3):1186–1198, 2010.

[31] L. V. Kantorovich and G. P. Alkilov. *Functional Analysis*. Nauka, Moskow, 1977.